IEEE Photonics Journal
An IEEE Photonics Society Publication

Open Access

Fabrication and Characterization of Dual Functional InGaN LED Arrays as the Optical Transmitter and Receiver for Optical Wireless Communications

Volume 13, Number 2, April 2021

Chia-Lung Tsai
Tong-Wen Wang
Yi-Chen Lu
Atanu Das
Sheng Hsiung Chang
Sun-Chien Ko

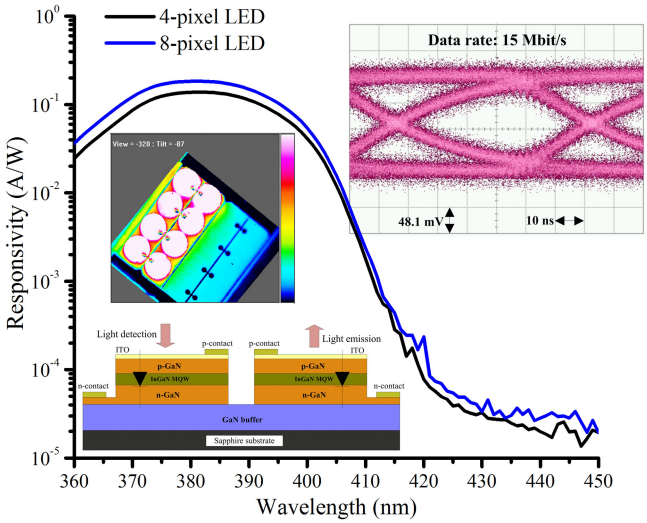

Optical wireless communications with the single-chip integrated transmitter and receiver

DOI: 10.1109/JPHOT.2021.3069841

Fabrication and Characterization of Dual Functional InGaN LED Arrays as the Optical Transmitter and Receiver for Optical Wireless Communications

Chia-Lung Tsai,[1,2] **Tong-Wen Wang**,[3] **Yi-Chen Lu**,[1] **Atanu Das**,[4] **Sheng Hsiung Chang**,[5] **and Sun-Chien Ko**[6]

[1]Department of Electronic Engineering and Green Technology Research Center, Chang Gung University, Taoyuan 33303, Taiwan
[2]Department of Otolaryngology-Head and Neck Surgery, Chang Gung Memorial Hospital, Taoyuan 33303, Taiwan
[3]Department of Electronic Engineering, Feng Chia University, Taichung 40724, Taiwan
[4]Zhejiang University, Zhejiang 310027, China
[5]Department of Physics, Chung Yuan Christian University, Taoyuan 33303, Taiwan
[6]Advanced Tech. Research Lab., Telecommunication Lab., Chunghwa Telecom Co., Ltd., Taoyuan 33303, Taiwan

DOI:10.1109/JPHOT.2021.3069841

Manuscript received March 3, 2021; revised March 19, 2021; accepted March 26, 2021. Date of publication March 30, 2021; date of current version April 13, 2021. This work was supported in part by the Ministry of Science and Technology (Taiwan) under Grants MOST 108-2221-E-182-055, MOST 107-2221-E-182-046, and MOST 106-2221-E-182-047 and in part by Chang Gung Memorial Hospital, Linkou under Grants BMRP 999 and CMRPD2K0201. Corresponding author: Chia-Lung Tsai (e-mail: cltsai@mail.cgu.edu.tw).

Abstract: The feasibility of using InGaN/GaN multiple-quantum-well light-emitting diode arrays (LED arrays) as photodiodes (PDs) is investigated experimentally in addition to their light emitting function. Two discrete LED arrays are produced from one 4×4 LED array with a parallel-connected pixel configuration. Such compact designs are useful for light emission or detection at the transmitting/receiving terminals of optical wireless communication systems. Despite 4×2 LED arrays achieving a light output power of 67.4 mW at 250 mA, they exhibit an optical responsivity (detectivity) of 0.183 A/W (1.61×10^{12} cm $Hz^{1/2}W^{-1}$) under ultraviolet light illumination ($\lambda = 380$ nm) at zero bias. For 4×2 LED arrays, the presence of an appreciable ultraviolet light response, together with a high 3-dB bandwidth ($\sim$8 MHz) for modulated light detection, allowed us to build a 15 Mbit/s directed optical link with these LEDs functioning as both the optical transmitter and the receiver. Finally, the unitary LED array-based optical link is capable of real-time transmission of digital audio signals (data rate = 6 Mbit/s) at a propagation distance of 100 cm in free space even though some of the constituent pixels are inactive for light detection.

Index Terms: InGaN, LED array, photodiode, optical wireless communications.

1. Introduction

With advances in manufacturing processes, including the use of a low-dimensional light-emitting medium with high spontaneous emission rate [1], a plasmonic nanostructure for light extraction improvement [2] and a novel wafer-scale packaging technique [3], solid-state lighting based

upon GaN-based light-emitting diodes (LEDs) has emerged as the dominant technology for indoor/outdoor illumination, horticulture/car lighting, and advertising displays. For these visible LEDs, InGaN/GaN multiple quantum wells (MQWs) grown on sapphire substrates are generally used as the active layer for light emission. However, due to the insulating property of the growth substrates, nonuniform light intensity distributions are commonly observed on top surface of InGaN LEDs due to the lateral transport of injection currents [4]. The phenomenon of current crowding in InGaN LEDs can be effectively addressed through optimizing the p-electrode patterns to facilitate uniform current spreading over the p-mesa region [5]. Besides, the pixelated LEDs provide an alternative way to alleviate the current crowding effect by dividing a large-size LED chip into several small pixels connected in serial or parallel [6], [7]. In addition to effectively transferring the heat energy from each pixel to the surrounding materials [8], the light extraction efficiency of these LED arrays can also be improved due to increased mesa sidewall area for light emissions [6]. Further study has been conducted by reducing the LED dimension to lower the internal electric field of InGaN MQWs to increase the LED's emission efficiency [9]. Therefore, despite functioning as an LCD backlight, pixelated LEDs are now considered as a potential candidate for use in next-generation displays [10].

Although the dynamic behavior of InGaN LEDs is mostly limited by the impact of spontaneous emission on carrier lifetime, tens to hundreds of MHz 3-dB modulation frequency can still be achieved, thus allowing for LED-based optical wireless communications [6], [7], [11], [12]. On the other hand, Yang *et al*. reported that p-i-n InGaN/GaN MQW LEDs that behave like photodiodes (PDs) under light illumination due to presence of an electrical field at the *pn* junction facilitates the extraction of photogenerated carriers from MQWs [13]. With the monolithic p-i-n PD and LED, a warning system has been proposed for UV light detection [14]. In optical wireless transmissions, the use of these PD-like LEDs can realize low-cost communication systems in which the InGaN MQW LEDs are simultaneously used as the optical transmitter and receiver. Gao *et al*. reported that full-duplex light communication at a transmission rate of 30 Mbps can be achieved by using a on-chip photonic circuit composed of the suspended waveguide, a ring resonator and two diodes with the same InGaN/GaN MQWs [15]. Using the InGaN/GaN MQWs to provide light emission from the LEDs and detection from the PDs, a 250 Mbit/s on-chip optical link with the LEDs, PDs and the waveguides has also been successfully realized [16]. Shrinking the device size down to micrometer scale, InGaN/GaN MQW-based micro-photodetectors (μPDs) are proposed as a high-speed optical receiver for Gbit/s visible light communications (VLC) [17]. Using the semipolar InGaN/GaN μPD as the photoreceiver and a 405 nm laser diode (LD) as the transmitter, a 1 m long VLC link capable of data transmission at a rate of 1.55 Gbit/s has also been proven through a simple non-return-to-zero on-off keying modulation scheme [18].

In this study, two discrete LED arrays integrated on a single chip were made from one 4 $\times$ 4 LED array with a parallel-connected pixel configuration. Such a compact design is useful for light emission or detection at the transmitting/receiving terminals of optical wireless communication systems. Instead of using different wavelengths to build the downstream and upstream data links [19], full (half)-duplex optical wireless communications could also be performed using the proposed optical transceiver integrated with the transmitter and receiver provided the LED arrays can detect the modulation light. The static and dynamic response of the LED arrays was experimentally assessed to clarify their capacity for use as PDs. Although improved 3-dB bandwidth for modulated light detection can be achieved by decreasing the pixel number of the PD-like LED arrays, they suffer from simultaneous degraded optical response and detectivity in the ultraviolet (UV) light range. Through the use of the parallel-connected pixel configuration, the system performance of an optical link with the unitary LED arrays can still work normally even if some of the constituent pixels for light detection are inactive. Finally, a 6 Mbit/s on-off keying based optical link capable of real-time transmission of digital acoustic signals is accomplished using two structurally identical LED arrays respectively functioning as the transmitter and receiver.

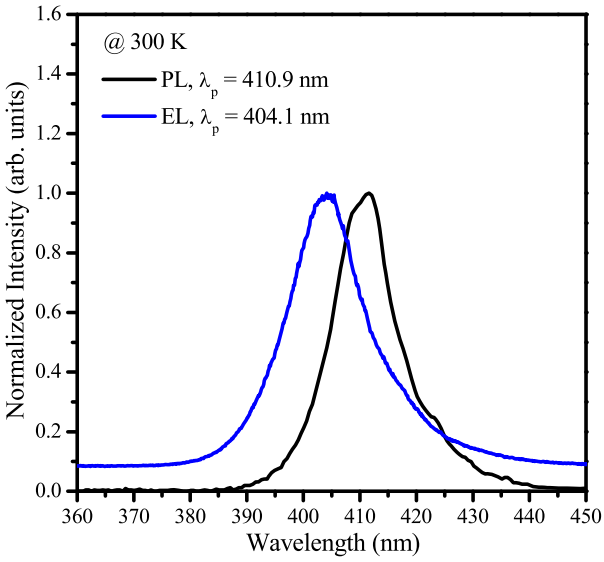

Fig. 1. The PL spectrum of the LED wafers used. The EL spectrum of 4 × 2 LED arrays operating at 100 mA is also shown for comparison.

2. Experiment

The LED epiwafers used herein were purchased from Formosa Epitaxy Inc. The LED epistructure grown on the patterned sapphire substrates consists of a GaN nucleation layer, a GaN buffer layer, a Si-doped GaN, an InGaN/GaN MQW, a p-AlGaN electron blocking layer, and the Mg-doped GaN layer. High-resolution X-ray diffraction (HRXRD), photoluminescence (PL) and electroluminescence (EL) measurements were used to verify the structural and optical properties of the LED wafers. The InGaN LEDs had a PL peak at $\lambda \sim 410.9$ nm and a full width at half maximum of 14.5 (shown in Fig. 1). In addition, the repeat period and the average indium composition of the InGaN MQWs are calculated as about 11.6 nm and 1.3% using the HRXRD.

After epitaxial growth, the pixelated LED design is used to relieve the current crowding effect, which is commonly observed in lateral InGaN LEDs. In this study, a simple SU-8 planarization was performed before the p-contact metallization process so that the individual pixels can be easily connected in parallel. Owing to its excellent mechanical and chemical stability, high aspect ratio feature and inherently insulating property [20], SU-8 is extremely suitable for use as a gap-filling material [21]. Details about the manufacturing procedures of the SU-8 planarized LED arrays can be found in our previous report [6]. According to the magnitude of the calculated current spreading length ($Ls \sim 239$ μm), which represents the uniformity of the distribution of injected carriers on the ITO-coated mesa, the diameter of each pixel is set at about 214 μm. Considering the LED reliability, the parallel-connected design of the constituent pixels is useful for the LED arrays because these LEDs can still work normally when some of the emitting pixels are inactive [6]. On the other hand, the discrete LED arrays can also be easily made from one LED array with the parallel-connected pixel configuration (i.e., through breaking the p-interconnect metals). This allows us to realize an optical transceiver (Fig. 2) with two 4 × 2 LED arrays (known as the single-chip integrated transmitter and receiver), one of which is used as the optical transmitter while the other is used as the receiver. Based upon the equivalent electric circuit of the proposed optical transceiver (i.e., two identical InGaN MQW LEDs), an optical data link can be built by respectively placing these transceivers at the transmitting terminal and receiving end. In addition to a filling of band-tail states, free-carrier screening of polarization fields in InGaN MQWs is considered responsible for the blueshift of the emission peak relative to PL peak position as 4 × 2 LED arrays operating at 100 mA [22]. By relieving the current crowding effect, the light can be uniformly emitted from each

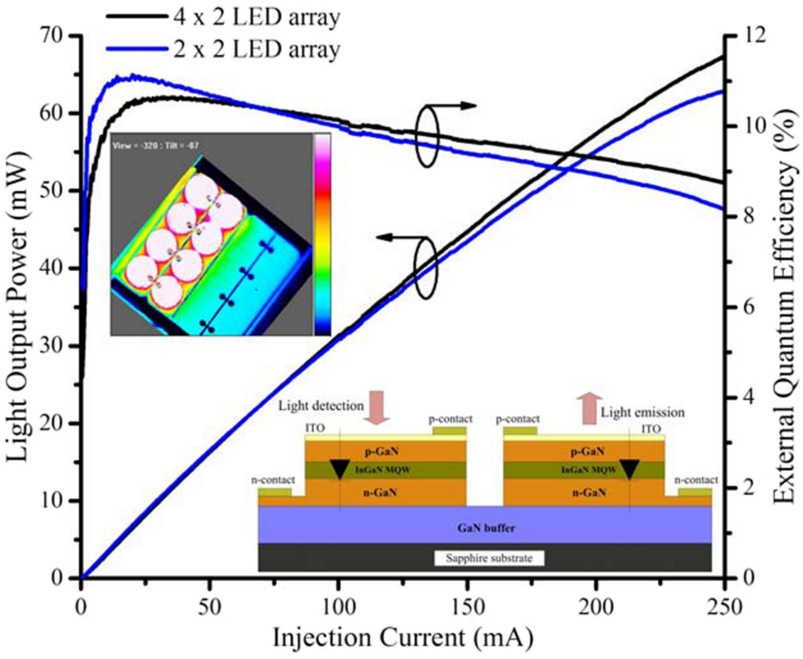

Fig. 2. The dependency of injection current on light output power and external quantum efficiency of the LED arrays with different emitting pixels. The inset shows the optical microscope image of the proposed optical transceiver (left up) and the corresponding equivalent electric circuit (right down). A uniform light distribution is observed for each pixel in one of 4 × 2 LED array operating at 100 mA.

pixel when one of the LED arrays is operating at 100 mA. To clarify the impact of the inactive pixels on device performance, the PD-like LED arrays were further fabricated with different numbers of pixels (i.e., 8 and 4 pixels) for light detection while the LED emitters used 8 pixels. The light output performance of the TO-packaged LEDs was characterized by a Keithley Model 2400 source meter and a calibrated integrating optical sphere sensor (Newport Corp.) In addition, the spectral response and the external quantum efficiency (EQE) of the PD-like LED arrays were measured by a detector responsivity measurement system (DSR100, Zolix) with a 75-W tungsten halogen lamp, monochromator, chopper and lock-in amplifier, and calibrated by a standard Si PD (DSR-A1, Zolix).

3. Results and Discussion

Fig. 2 shows the dependency of injection current on the light output power and external quantum efficiency of the LED arrays with different emitting pixels. As a result of reduced pixel number in the LED arrays with a parallel-connected pixel configuration, the forward voltage and the equivalent series resistance slightly increased from 3.09 V and 5.4 Ω (for 4 × 2 LED array) to 3.22 V and 9.6 Ω (for 2 × 2 LED array). In addition, the maximum light output power and the external quantum efficiency of the 8- and 4-pixel containing LED arrays are respectively evaluated as 67.4 mW (@ I = 250 mA) and 10.5% (@ I = 20 mA), and 62.9 mW (@ I = 250 mA) and 11.1% (@ I = 14 mA). At a low current injection level, light intensity is proportional to the injection current in the fabricated LED arrays and then the emission efficiency is degraded by Joule heating and/or carrier density-dependent Auger recombination as the LEDs operate at elevated current levels [23]. For 2 × 2 LED arrays, the increased current density for each emitting pixel is responsible for their effective light emission at lower current levels, even though these LEDs suffer from more apparent efficiency droop at high currents.

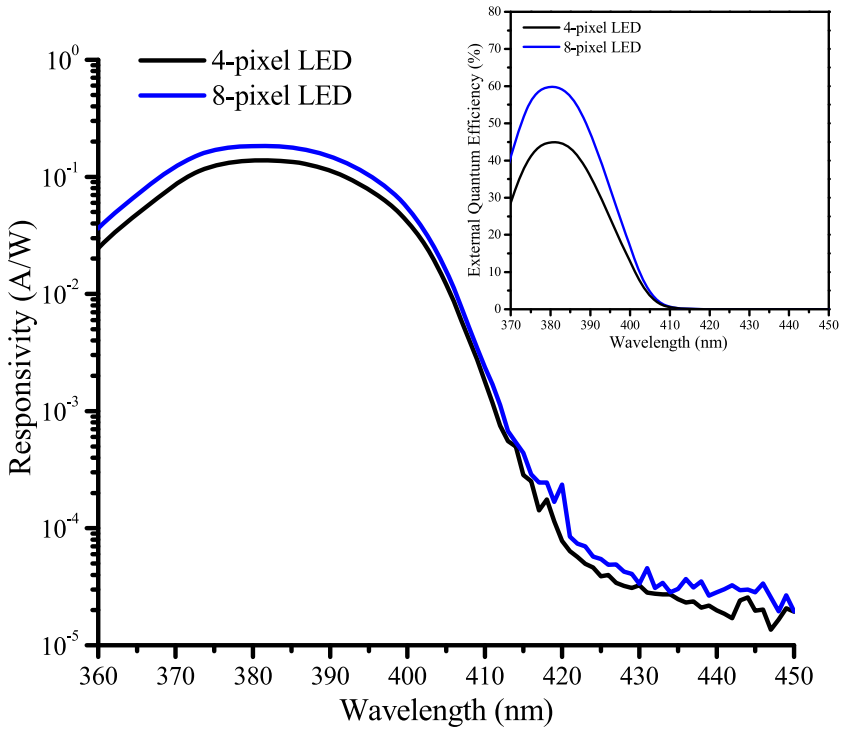

Fig. 3. The spectral responsivity and quantum efficiency of the LED arrays with different constituent pixels for optical absorption.

TABLE 1
Optoelectrical Characteristics of the LED Arrays With Different Pixels for Optical Absorption.

Sample	Peak R_λ (A/W) @ 0 V	Peak EQE (%)	R(380 nm)/R(450 nm) @ 0 V
4-pixel LED	0.137	44.8	7084
8-pixel LED	0.183	59.9	9366

Fig. 3 shows the spectral responsivity and the corresponding external quantum efficiency of 4 $\times$ 2 LED arrays with different constituent pixels for optical absorption. The optoelectrical characteristics of the fabricated LED arrays are summarized in Table 1. The peak responsivity and the external quantum efficiency of 4 $\times$ 2 LED arrays at zero bias are higher than those of 2 $\times$ 2 LED arrays. A responsivity ratio improvement from 380 nm relative to 450 nm (referred as UV/visible rejection ratio) is also found in 4 $\times$ 2 LED arrays. This result is attributed to an increased light absorption area in the 4 $\times$ 2 LED arrays as these LED arrays were measured under the same illumination conditions. For both LEDs, the discernible optical absorption starts at $\lambda = 450$ nm, with increased responsivity (external quantum efficiency) and a decreasing wavelength until $\lambda \sim 390$ nm, at which point the available quantum efficiency diminishes as the wavelength of the incident light falls below 375 nm. For InGaN MQWs, the presence of the indium compositional fluctuation and the quantum confined Franz-Keldysh (QCFK) effects is seen as responsible for a large shift of the PL peak relative to the InGaN-related absorption edge [24]. This results in the slow response of the optical absorption with wavelengths ranging from 450 nm to 410 nm. In addition, optical absorption via

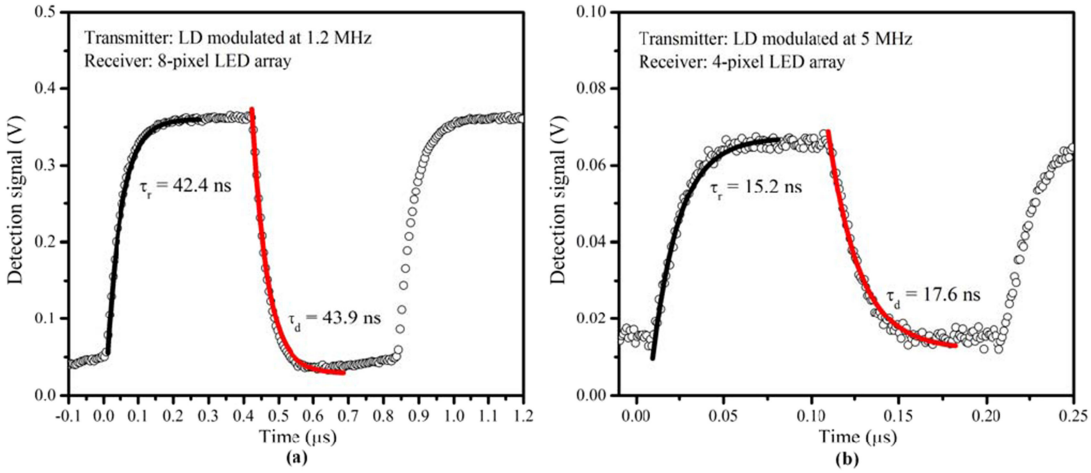

Fig. 4. Transient response of (a) 4 × 2 and (b) 2 × 2 LED arrays at zero bias and illuminated by a commercial near-ultraviolet LD with a modulation frequency (square wave) of 1.2 MHz and 5 MHz, respectively. During measurements, the LD was pre-biased at 30 mA.

the transition from the Mg-related states to the conduction band of the p-GaN within the space-charge region should also contribute to the peak responsivity at $\lambda \sim 380$ nm [25]. As a result of the ITO-induced optical absorption and strong surface recombination [14], [26], the optical conversion efficiency is apparently degraded at shorter wavelengths ($\lambda < 375$ nm). On the other hand, the output performance of the PDs can be further characterized by the normalized detectivity (D^*). It is defined as $D^* = R_\lambda/(2qJ_d)^{1/2}$, where R_λ is the responsivity, J_d is the dark current density of the detector and q is the electron charge (1.6×10^{-19} C) [27]. For 4 × 2 LED arrays, the estimated detectivity at an incident wavelength of 380 nm is approximately 1.61×10^{12} cm $Hz^{1/2}W^{-1}$ at zero bias, which is comparable to that of GaN-based ultraviolet PDs [28]. This indicates that the 4 × 2 LED arrays can not only being used as conventional semiconductor light sources but they can also be suited for the detection of ultraviolet light.

Fig. 4 shows the transient response of the 4 × 2 and 2 × 2 LED arrays illuminated by a commercial near-UV LD. Despite being biased at DC current of 30 mA, the LD was also modulated by a square waveform with a peak-to-peak voltage (V_{PP}) of 2 V and an offset voltage of 0 V. In addition, the tiny photocurrent generated from the LED arrays was amplified by a 33 dB amplifier (THS4271, Texas Instruments) and read out using a digital oscilloscope (DSO-X 3034A, Agilent). A good switching property of the detection signals, corresponding to the high/low light output state of the modulated LDs, is clearly observed as the LD was modulated at 1.2 MHz (5 MHz) while the 8-pixel (4-pixel) containing LED array was used for light detection. The rise time (τ_r) and fall time (τ_d) can be described and fitted by the following equations [28]:

$$V = V_0\left[1 - \exp\left(-\frac{t}{\tau_r}\right)\right] \tag{1}$$

$$V = V_0 \exp\left(-\frac{t}{\tau_d}\right) \tag{2}$$

where V_0 is the maximum photovoltage at time t. By fitting the experimental data to the equations (1) and (2), the τ_r and τ_d are respectively calculated as 42.4 ns and 43.9 ns, and 15.2 ns and 17.6 ns for the 4 × 2 and 2 × 2 LED arrays. Therefore, the maximum 3-dB cut-off frequency of the 4 × 2 and 2 × 2 LED arrays (zero bias) under the modulated light detection can be respectively

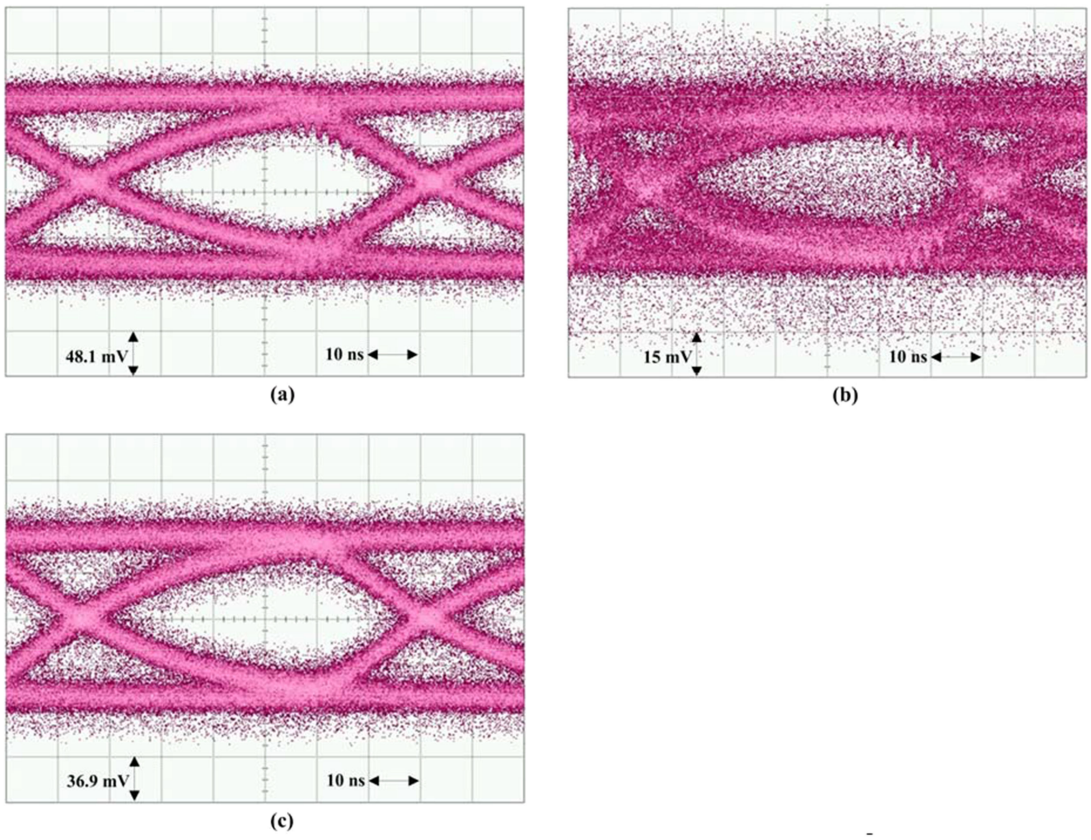

Fig. 5. Eye diagram measured at 15 Mbit/s and pseudo random bit sequence pattern of 2^7–1 for the LED-based optical link with a 4 × 2 LED transmitter operating at $I_{Bias} = 220$ mA and $V_{PP} = 5$ V and a PD-like LED array (zero bias) using (a) 8, (b) 4, and (c) 6 pixels for light detection. The used optical link is identical to that shown in Fig. 6(a).

estimated as 8 MHz and 19.9 MHz according to the following relationship [29]:

$$f_{3dB} = \frac{2.20}{2\pi\tau_d} \tag{3}$$

Similar experimental setup including the bias tee-driven LD transmitter ($\lambda = 404$ nm & $I_{Bias} = 70$ mA), light coupling lens (two plano-convex lenses), and the Rohde & Schwarz ZVL network analyzer was used to investigate the dynamic response of the PD-like LED arrays. In the experiment, the trend of the increased 3-dB frequency bandwidth with decreasing the pixel number of the PD-like LED arrays (i.e., $f_{3dB} = 5.2$ MHz and 17.6 MHz for the 4 × 2 and 2 × 2 LED receivers biased at 0 V) is the same as their transient response analysis. The higher modulation bandwidth in the LED arrays with fewer pixels (4 pixels) for light detection could be attributed to a decrease in the resistance-capacitance (RC) delay time as the number of the parallel-connected pixels is reduced [30].

Using the p-i-n InGaN/GaN MQW LED structures for light detection, the fabricated LED arrays indeed exhibit PD-like behaviors in the UV light range. In addition, the available 3-dB bandwidth for modulated light detection is also as high as 19.9 MHz (depending on the number of pixels in the LED arrays). Both unique features make them potentially useful for the LED-based optical wireless transmission system. Therefore, the feasibility of using these devices as an optical receiver is experimentally investigated. Fig. 5 shows the eye diagram measured at 15 Mbit/s for an optical

link with two 4 × 2 LED arrays respectively functioning as the transmitter and receiver. To facilitate efficient energy utilization, two plano-convex lenses (Edmund Optics, 40.0 mm Dia. × 60.0 mm FL uncoated plano-convex lens) with convex surfaces facing each other were introduced into the optical link [31]. The light coupling efficiency (η) in such a directed optical link is calculated to be about 37% at a light propagation distance of 10 cm. During measurements, the bias current (I_{Bias}) together with the test signals (nonreturn-to-zero pseudorandom bit sequence generated from an Agilent 81160A pulse function arbitrary noise generator) were combined via a high-frequency bias tee and fed to the TO-packaged LED array (4 × 2 pixels). The modulated light from the LED will propagate through a moderate distance (L = 10 cm) in free space and is then detected by the PD-like LED arrays connected to a 33 dB amplifier (THS4271, Texas Instruments). Finally, the amplified electrical signals were characterized using a wide-bandwidth sampling oscilloscope (Agilent 86100A). As shown in Fig. 5, the eye diagram of proposed optical link with a 4 × 2 LED emitter operating at 15 Mbit/s with I_{Bias} = 220 mA and 2^7-1 word length (pseudorandom bit sequence) shows a clear and opening feature with peak-to-peak jitter below 25 ps as an 8-pixel containing LED array was used for light detection. After inspecting the received data stream with a series of training symbols from the real-time oscilloscope (Agilent, DSO-X 3034A), we also find that all transmitted digital signals relative to the original ones were well preserved at the receiving end, using an 8- or 6-pixel containing LED array for light detection. These results suggest that the proposed optical wireless communication system is capable of 15 Mbit/s data transmission over a distance of 10 cm in free space. In addition, the transmission performance of such optical links is also comparable to that of in-plane visible light communications with the monolithically integrated InGaN MQW LED/PD [32]. It is known that the system performance of optical wireless communications is not only correlated with the 3-dB bandwidth of the optical links, but the magnitude of the electrical signals given from the PDs also plays an important role [33]. The system bandwidth of the proposed optical link could be enhanced by decreasing the pixel number of the 4 × 2 LED emitters because the constituent pixels were connected in parallel [34]. It should be noted that the lowering of the signal-to-noise ratio (SNR) associated with the reduced optical signal level of the receiver can be alleviated by increasing the LED bias current. The performance of the LED-based light communication systems can be further improved by using an adequate modulation scheme such as the multi-band orthogonal frequency division multiplexed (OFDM) modulation [35] or the color-shift-keying embedded direct-current optical-orthogonal-frequency-division-multiplexing (CSK-DCO-OFDM) modulation [36]. In addition, shrinking the device dimension (e.g., micro PDs) to lower the RC delay time is also useful for achieving high-speed light detection [37]. On the other hand, the eye diagram becomes fuzzy, accompanied by numerous bit errors at the receiving end (not shown here) under the same measurement conditions when the number of pixels in the PD-like LED arrays is reduced to 4. Although 2 × 2 LED arrays can detect the modulated light at relatively high frequencies (i.e., f_{3dB} = 19.9 MHz), the decrease in the effective light absorption area accompanied by the reduced photocurrent under illumination results in degraded system performance in the proposed optical link using these PD-like LED arrays. This is supported by the improved eye diagram quality achieved by increasing the number of pixels from 4 to 6, as shown in Fig. 5(c). To address this issue, the 4 × 2 LED emitter can be replaced by a near-UV LD to increase the light coupling efficiency of the directed optical links with two plano-convex lenses respectively placed in front of the transmitter and the receiver. As a result of the improved SNR at the receiving end, the eye diagram has clear and open eyes at 25 Mbit/s (not shown here). In such an optical link with an LD transmitter and a 2 × 2 LED receiver, the value of the bit-error-rate (BER) is evaluated as 3.2 × 10^{-5}. However, when a 4 × 2 LED array was used as the receiver the eye diagram quality degrades significantly accompanied with an increased BER (∼9.7 × 10^{-2}) even for the lowest data rate of 21 Mbit/s [the minimum clock frequency of the BER tester (Agilent E4861B)]. This is consistent with the result given from the transient response of the PD-like LED arrays under UV light illumination (Fig. 4).

A practical implementation of an optical wireless communication system capable of wirelessly transmitting/receiving audio signals was produced using the unitary LED arrays as transmitter and receiver. Fig. 6 shows the experimental setup of an optical link used for real-time transmissions

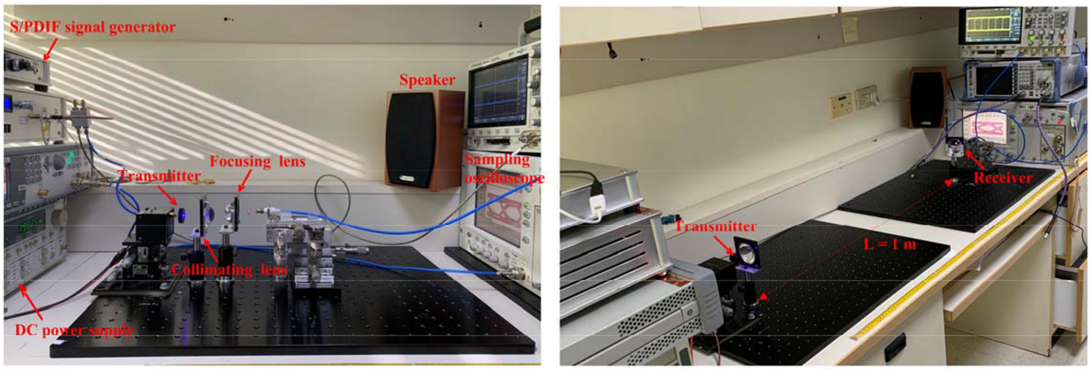

Fig. 6. Experimental setup of the LED-based optical wireless link for real-time transmissions of the S/PDIF acoustic signals. A 4 × 2 LED array operated at I_{Bias} = 200 mA and an 8-pixel containing LED biased at zero voltage were respectively used as the optical transmitter and receiver. The sound can be distinctly heard from the speaker even as the distance between the transmitter and the receiver was increased from (a) 10 cm to (b) 100 cm.

of digital audio signals. In the transmitting terminals, computer-readable recording media such as the waveform audio format (WAV) files was processed using a commercial S/PDIF converter to generate the digital audio signals with the S/PDIF format. S/PDIF (Sony Philips Digital Interface) is a widely adopted format in home media entertainment devices [38]. The 4 × 2 LED emitter pre-biased at 200 mA was directly modulated by the S/PDIF audio signals. The modulated light in free space was guided towards the receiver using a directed optical link with the collimating and focusing lenses in front of the transmitter and the receiver. At the receiving end, the receiver comprised of a 4 × 2 LED array connected with a 33 dB amplifier (THS4271, Texas Instruments), a S/PDIF decoder (CS8416, Cirrus Logic) and a digital-to-analog converter (CS4398, Cirrus Logic) was used to recover the original audio signals and the sound is then output using a speaker. The light coupling efficiency of such a communication system is estimated at 37% (36.2%) at a propagation distance of 10 cm (100 cm). After careful inspection of the data streams of the original S/PDIF acoustic signals relative to the received signals (Fig. 7), we found that all transmitted bits can be well preserved at the receiving end (i.e., a loud and clear song can be heard from the speaker) using an optical link between the transmitter and receiver. In addition, real-time transmissions of digital audio signals have been shown to be feasible even with data transmitted at a propagation distance of 100 cm. With the parallel-connected pixel design, the proposed data transmission system can still work normally even for light detection with 6 pixels, consistent to the results shown in Fig. 5. It should be noted that, due to the presence of the crosstalk effects between the neighboring LED arrays [39], the outward and return signals can not be communicated at the same time in our communication systems. This issue could be addressed by building a half-duplex time-division duplexing (HD-TDD) communication system, as reported in Ref. [40].

4. Conclusion

In summary, the parallel-connected design of the constituent pixels is proposed to fabricate the InGaN LEDs with uniform light emission patterns. By breaking the metal interconnects, two discrete LED arrays on the same chip can also be easily made from one LED array with a parallel-connected pixel configuration. This allows us to realize an optical transceiver composed of a LED transmitter and a PD-like LED receiver. As a result of increased effective area for light detection, the optical responsivity and detectivity of 4 × 2 LED arrays at zero bias is superior to that obtained using a 4-pixel containing LED even though their capacity for modulated light detection is restricted at low speeds (i.e., f_{3dB} = 8 MHz versus 19.9 MHz). Such a result is consistent with the finding that a

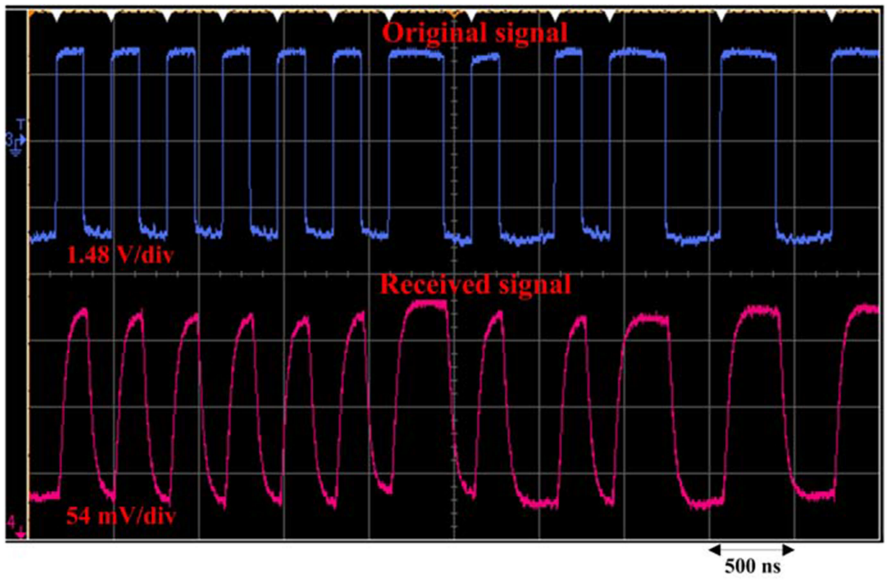

Fig. 7. Comparison of the data streams between the original S/PDIF acoustic signals and the received signals using a digital oscilloscope (Agilent, DSO-X 3034A). The bandwidth of the real-time oscilloscope is 350 MHz, with a vertical resolution of 8 bits at a sampling rate of 4 GSa/s. Two 8-pixel containing LED arrays were respectively used as the transmitter and receiver in the proposed optical link for real-time acoustic transmissions. The data rate is measured at 6 Mbit/s.

15 Mbit/s directed optical link can be obtained using a 4×2 LED emitter and a PD-like LED array with more than six pixels. Finally, real-time transmissions of digital audio signals (data rate $=$ 6 Mbit/s) at a propagation distance of 100 cm in free space were found to be feasible using the unitary LED array to create optical links with a simple on-off keying modulation scheme.

References

[1] J. J. Wierer, N. Tansu, A. J. Fischer, and J. Y. Tsao, "III-nitride quantum dots for ultra-efficient solid-state lighting," *Laser Photon. Rev.*, vol. 10, no. 4, pp. 612–622, May 2016.
[2] A. Fadil, Y. Ou, D. Iida, S. Kamiyama, P. M. Petersena, and H. Ou, "Combining surface plasmonic and light extraction enhancement on InGaN quantum-well light-emitters," *Nanoscale*, vol. 8, no. 36, pp. 16340–16348, Aug. 2016.
[3] K. T. Shimizu *et al.*, "Toward commercial realization of quantum dot based white light-emitting diodes for general illumination," *Photon. Res.*, vol. 5, no. 2, pp. A1–A6, Feb. 2017.
[4] X. Guo, Y. L. Li, and E. F. Schubert, "Efficiency of GaN/InGaN light-emitting diodes with interdigitated mesa geometry," *Appl. Phys. Lett.*, vol. 79, no. 13, pp. 1936–1938, Sep. 2001.
[5] H. Kim *et al.*, "Modeling of a gan-based light-emitting diode for uniform current spreading," *Appl. Phys. Lett.*, vol. 77, no. 12, pp. 1903–1904, Sep. 2000.
[6] C. L. Tsai, and C. T. Yen, "SU-8 planarized InGaN light-emitting diodes with multipixel emission geometry for visible light communications," *IEEE Photon. J.*, vol. 7, no. 1, Feb. 2015, Art. no. 1600109.
[7] H. Huang *et al.*, "Cascade GaN-based blue micro-light-emitting diodes for dual function of illumination and visible light communication," *J. Phys. D: Appl. Phys.*, vol. 53, no. 35, Jun. 2020, Art. no. 355103.
[8] Z. Gong *et al.*, "Size-dependent light output, spectral shift, and self-heating of 400 nm InGaN light-emitting diodes," *J. Appl. Phys.*, vol. 107, Jan. 2010, Art. no. 013103.
[9] J. Zhan *et al.*, "Investigation on strain relaxation distribution in GaN-based μLEDs by kelvin probe force microscopy and micro-photoluminescence," *Opt. Exp.*, vol. 26, no. 5, pp. 5265–5274, Mar. 2018.
[10] J. J. Wierer, and N. Tansu, "III-Nitride micro-LEDs for efficient emissive displays," *Laser Photon. Rev.*, vol. 13, no. 9, Sep. 2019, Art. no. 1900141.
[11] J. J. D. McKendry *et al.*, "Visible-light communications using a CMOS-controlled micro-light-emitting-diode array," *J. Lightw. Technol.*, vol. 30, no. 1, pp. 61–67, Jan. 2012.
[12] C. Shen *et al.*, "High-speed 405-nm superluminescent diode (SLD) with 807-MHz modulation bandwidth," *Opt. Exp.*, vol. 24, no. 18, pp. 20281–20286, Aug. 2016.
[13] H. Yang *et al.*, "The enhanced photo absorption and carrier transportation of InGaN/GaN quantum wells for photodiode detector applications," *Sci. Rep.*, vol. 7, Feb. 2017, Art. no. 43357.

[14] Y. C. Chiu, P. S. Yeh, T. H. Wang, T. C. Chou, C. Y. Wu, and J. J. Zhang, "An ultraviolet sensor and indicator module based on p–i–n photodiodes," *Sensors*, vol. 19, no. 22, Nov. 2019, Art. no. 4938.
[15] X. Gao *et al.*, "A 30 Mbps in-plane full-duplex light communication using a monolithic GaN photonic circuit," *Semicond. Sci. Technol.*, vol. 32, no. 7, 2017, Art. no. 075002.
[16] K. H. Li, Y. F. Cheung, W. Y. Fu, K. K. Y. Wong, and H. W. Choi, "Monolithic integration of GaN-on-sapphire light-emitting diodes, photodetectors, and waveguides," *IEEE J. Sel. Topics Quantum Electron.*, vol. 24, no. 6, Nov./Dec. 2018, Art. no. 3801706.
[17] K. J. Singh *et al.*, "Micro-LED as a promising candidate for high-speed visible light communication," *Appl. Sci.*, vol. 10, no. 20, Oct. 2020, Art. no. 7384.
[18] S. W. H. Chen *et al.*, "High-bandwidth green semipolar (20−21) InGaN/GaN micro light-emitting diodes for visible light communication," *ACS Photon.*, vol. 7, no. 8, pp. 2228−2235, Aug. 2020.
[19] G. Cossu, R. Corsini, and E. Ciaramella, "High-speed bi-directional optical wireless system in non-directed line-of-sight configuration," *J. Lightw. Technol.*, vol. 32, no. 10, pp. 2035–2040, May 2014.
[20] J. Lu *et al.*, "Effect of SU-8 passivation layer induced stress on the performance of GaSb diode," *IEEE Photon. Technol. Lett.*, vol. 30, no. 11, pp. 1060–1063, Jun. 2018.
[21] C. M. Kang *et al.*, "Fabrication of a vertically-stacked passive-matrix micro-LED array structure for a dual color display," *Opt. Exp.*, vol. 25, no. 3, pp. 2489–2495, Feb. 2017.
[22] C. Lu *et al.*, "Investigation of the electroluminescence spectrum shift of InGaN/GaN multiple quantum well light-emitting diodes under direct and pulsed currents," *J. Appl. Phys.*, vol. 113, no. 1, Jan. 2013, Art. no. 013102.
[23] J. Piprek, "Efficiency droop in nitride-based light-emitting diodes," *Phys. Status Solidi A*, vol. 207, pp. 2217–2225, Jul. 2010.
[24] Y. Zhang *et al.*, "Stokes shift in semi-polar (11–22) InGaN/GaN multiple quantum wells," *Appl. Phys. Lett.*, vol. 108, no. 3, Jan. 2016, Art. no. 031108.
[25] S. J. Chung, E. K. Suh, H. J. Lee, H. B. Mao, and S. J. Park, "Photoluminescence and photocurrent studies of p-type GaN with various thermal treatments," *J. Cryst. Growth*, vol. 235, no. 1-4, pp. 49–54, Feb. 2002.
[26] W. Yang, T. Nohova, S. Krishnankutty, R. Torreano, S. McPherson, and H. Marsh, "Back-illuminated GaN/AlGaN heterojunction photodiodes with high quantum efficiency and low noise," *Appl. Phys. Lett.*, vol. 73, no. 8, pp. 1086–1088, Aug. 1998.
[27] A. M. Chowdhury *et al.*, "Self-powered, broad band, and ultrafast INGaN-based photodetector," *ACS Appl. Mater. Interfaces*, vol. 11, no. 10, pp. 10418–10425, Feb. 2019.
[28] A. Gundimeda *et al.*, "Fabrication of non-polar GaN based highly responsive and fast UV photodetector," *Appl. Phys. Lett.*, vol. 110, no. 10, Mar. 2017, Art. no. 103507.
[29] E. Monroy, F. Omnès, and F. Calle, "Wide-bandgap semiconductor ultraviolet photodetectors," *Semicond. Sci. Technol.*, vol. 18, no. 4, pp. R33–R51, Mar. 2003.
[30] B. Alshehri *et al.*, "Dynamic characterization of III-nitride-based high-speed photodiodes," *IEEE Photon. J.*, vol. 9, no. 4, Aug. 2017, Art. no. 6803107.
[31] C. L. Tsai, Y. C. Li, Y. C. Lu, and S. H. Chang, "Fabrication and characterization of si substrate-free InGaN light-emitting diodes and their application in visible light communications," *IEEE Photon. J.*, vol. 9, no. 2, Apr. 2017, Art. no. 8200612.
[32] W. Cai *et al.*, "On-chip integration of suspended InGaN/GaN multiple-quantum-well devices with versatile functionalities," *Opt. Exp.*, vol. 24, no. 6, pp. 6004–6010, Mar. 2016.
[33] H. Li, X. Chen, J. Guo, Z. Gao, and H. Chen, "An analog modulator for 460 MB/S visible light data transmission based on OOK-NRS modulation," *IEEE Wireless Commun.*, vol. 22, no. 2, pp. 68–73, Apr. 2015.
[34] C. L. Tsai, Y. C. Lu, and S. H. Chang, "InGaN LEDs fabricated with parallel-connected multi-pixel geometry for underwater optical communications," *Opt. Laser Technol.*, vol. 118, pp. 69–74, Oct. 2019.
[35] C. H. Yeh, H. Y. Chen, C. W. Chow, and Y. L. Liu, "Utilization of multi-band OFDM modulation to increase traffic rate of phosphor-LED wireless VLC," *Opt. Exp.*, vol. 23, no. 2, pp. 1133–1138, Jan. 2015.
[36] W. H. Gunawan, Y. Liu, C. H. Yeh, and C. W. Chow, "Color-shift-keying embedded direct-current optical-orthogonal-frequency-division-multiplexing (CSK-DCO-OFDM) for visible light communications (VLC)," *IEEE Photon. J.*, vol. 12, no. 5, Oct. 2020, Art. no. 7905205.
[37] C. H. Kang *et al.*, "Semipolar (20–2–1) InGaN/GaN micro-photodetector for gigabit-per-second visible light communication," *Appl. Phys. Exp.*, vol. 13, no. 1, 2020, Art. no. 014001.
[38] D. K. Son, E. Cho, I. Moon, Z. Ghassemlooy, S. Kim, and C. G. Lee, "Simultaneous transmission of audio and video signals using visible light communications," *EURASIP J. Wireless Commun. Netw.*, vol. 2013, Oct. 2013, Art. no. 250.
[39] T. Kurosaki *et al.*, "1.3/1.55 μm full-duplex WDM optical transceiver modules for ATM-PON (PDS) systems using PLC-hybrid-integration and CMOS-IC technologies," *IEICE Trans. Electron.*, vol. E-82-B, no. 8, pp. 1199–1208, Aug. 1999.
[40] Y. F. Liu, C. H. Yeh, C. W. Chow, Y. Liu, Y. L. Liu, and H. K. Tsang, "Demonstration of bi-directional LED visible light communication using TDD traffic with mitigation of reflection interference," *Opt. Exp.*, vol. 20, no. 21, pp. 23019–23024, Sep. 2012.